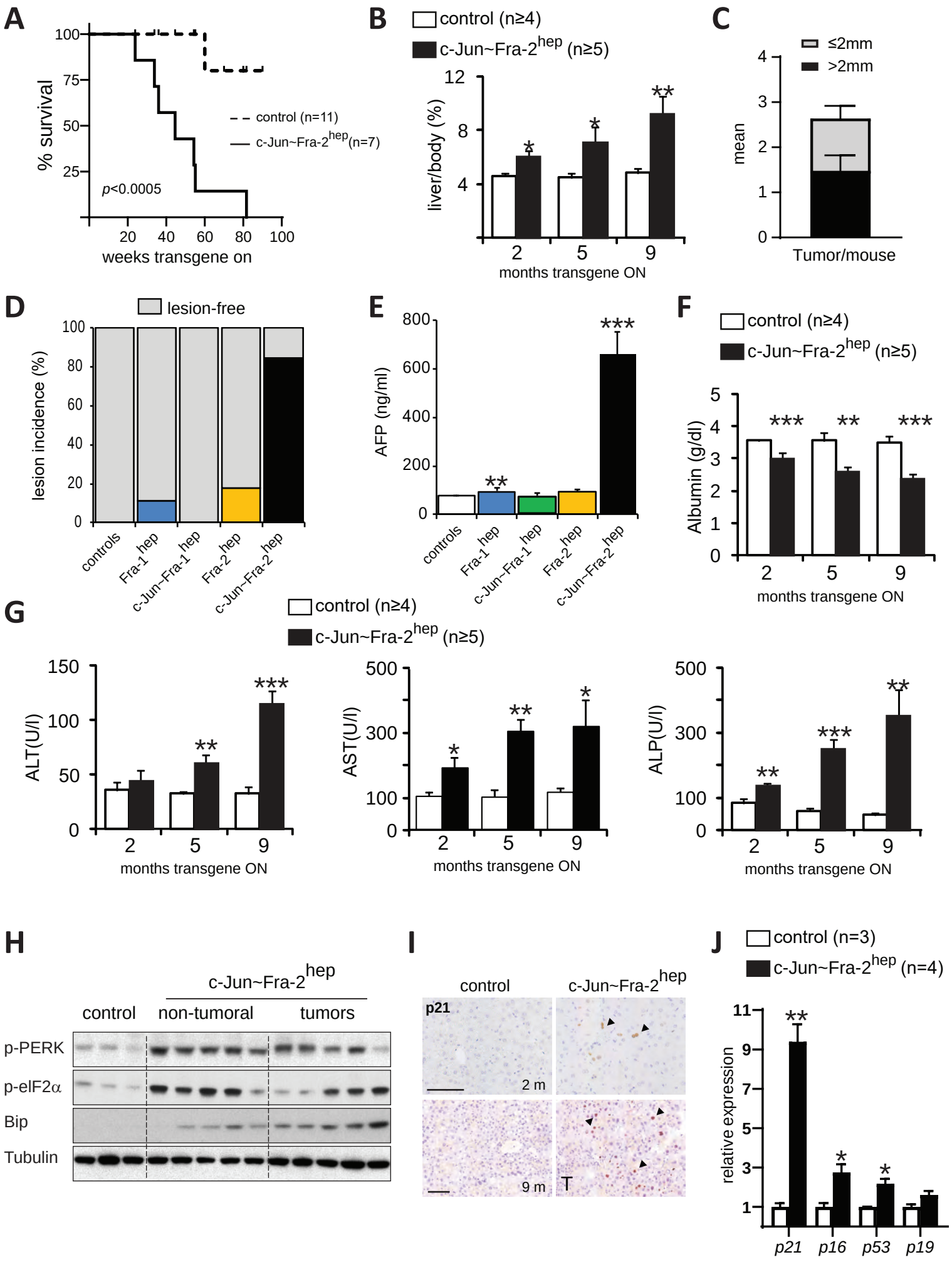

Sup Figure 1. Bakiri et al.

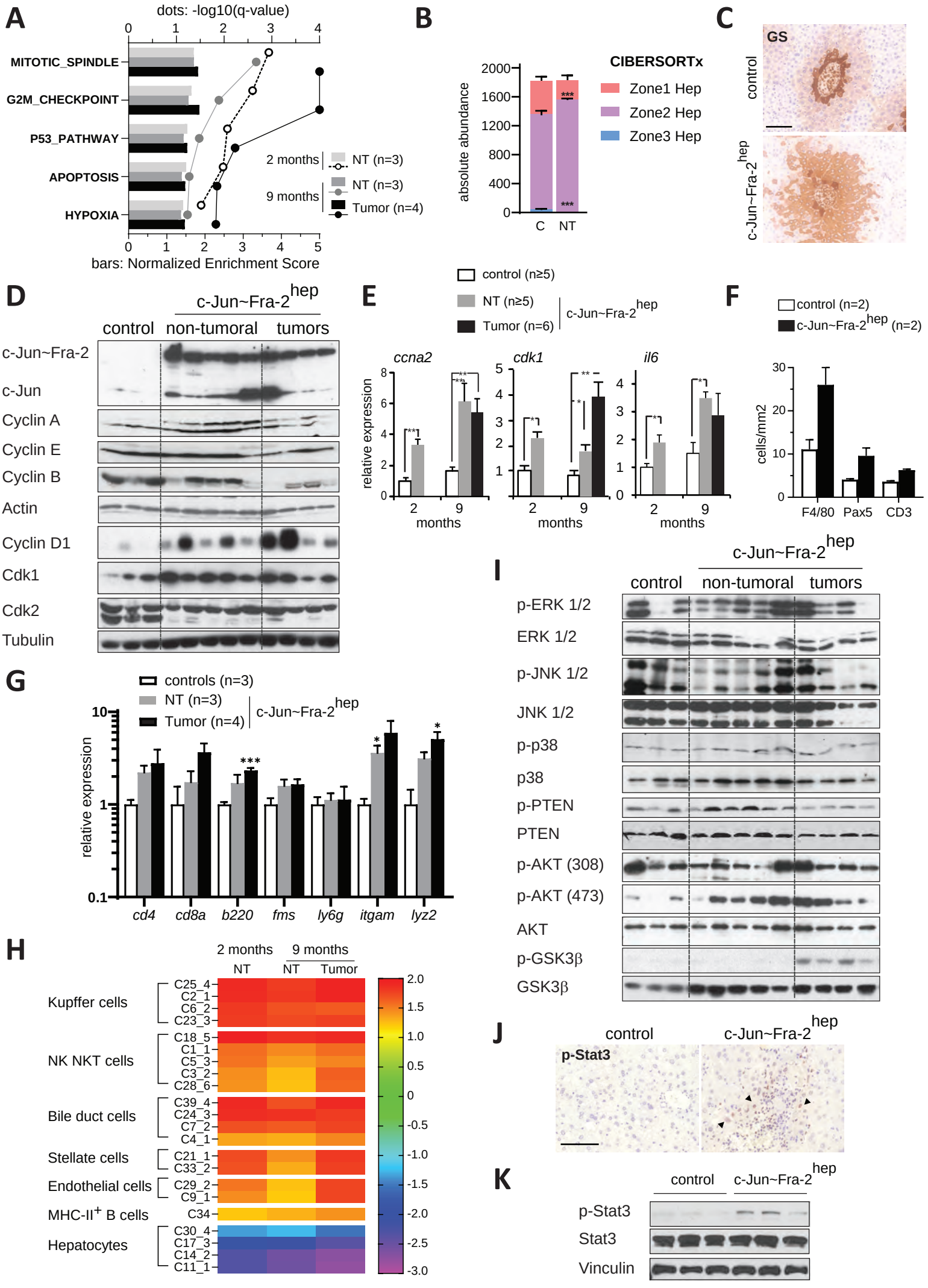

Sup Figure 2. Bakiri et al.

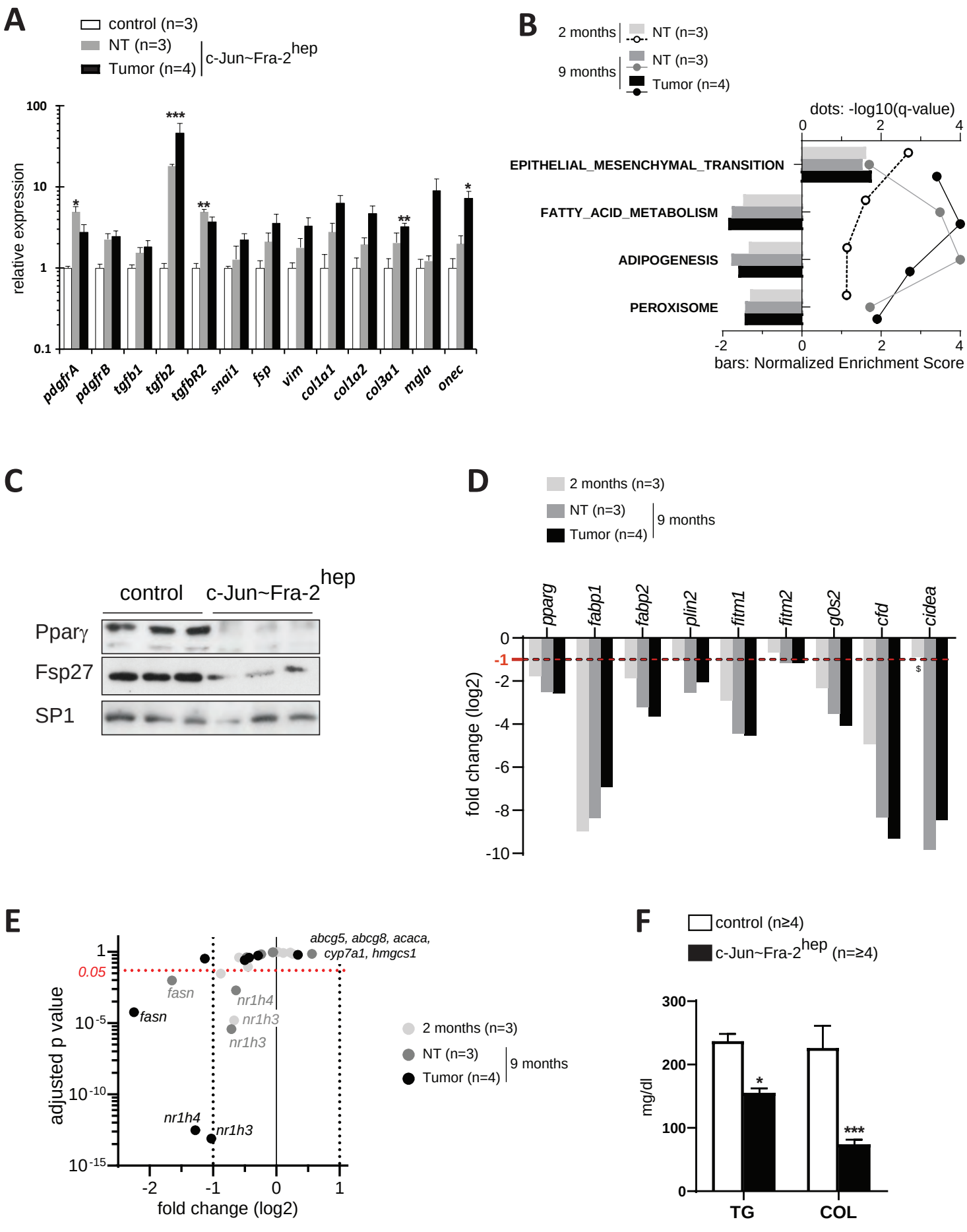

Sup Figure 3. Bakiri et al.

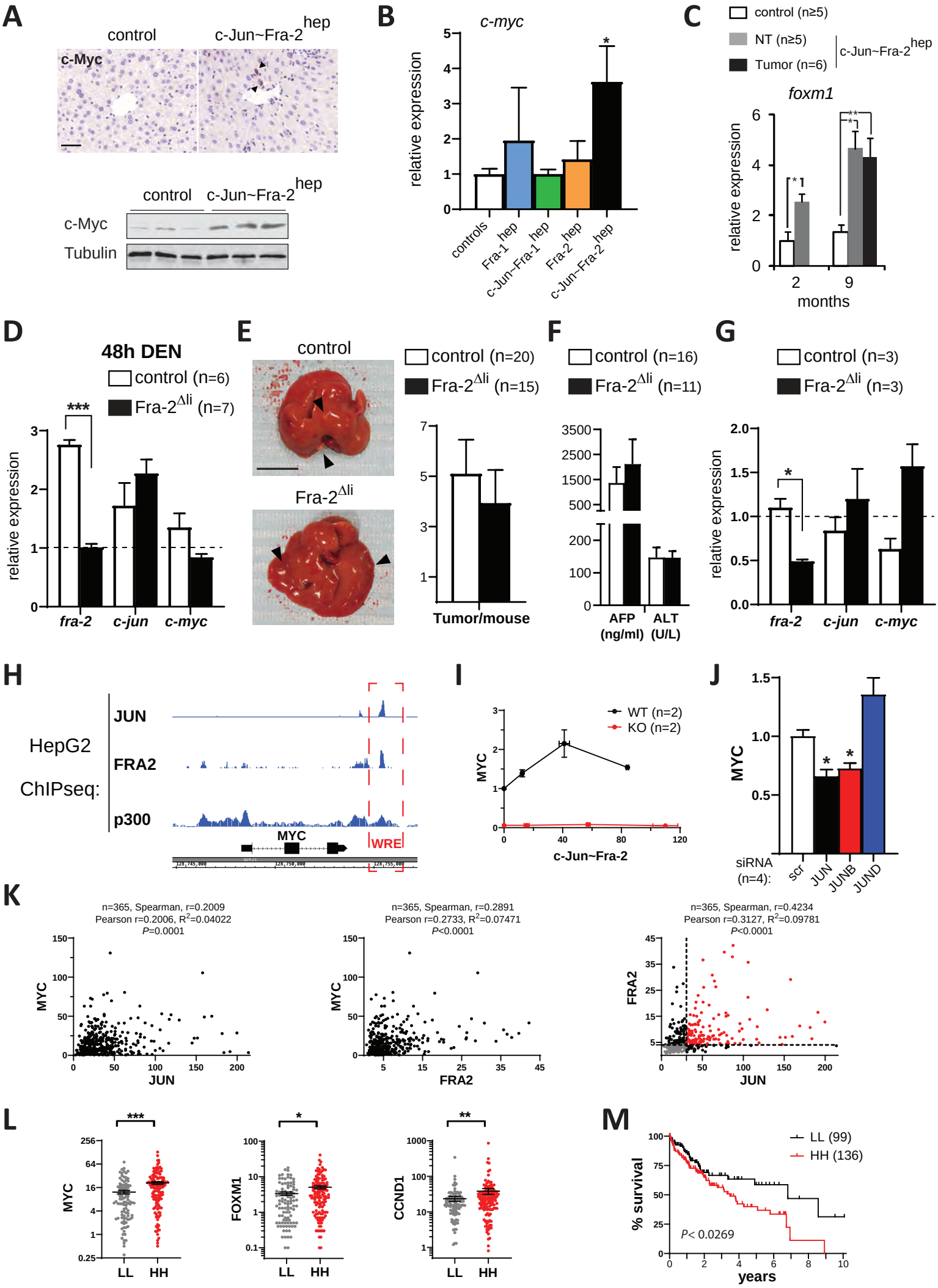

Sup Figure 4. Bakiri et al.

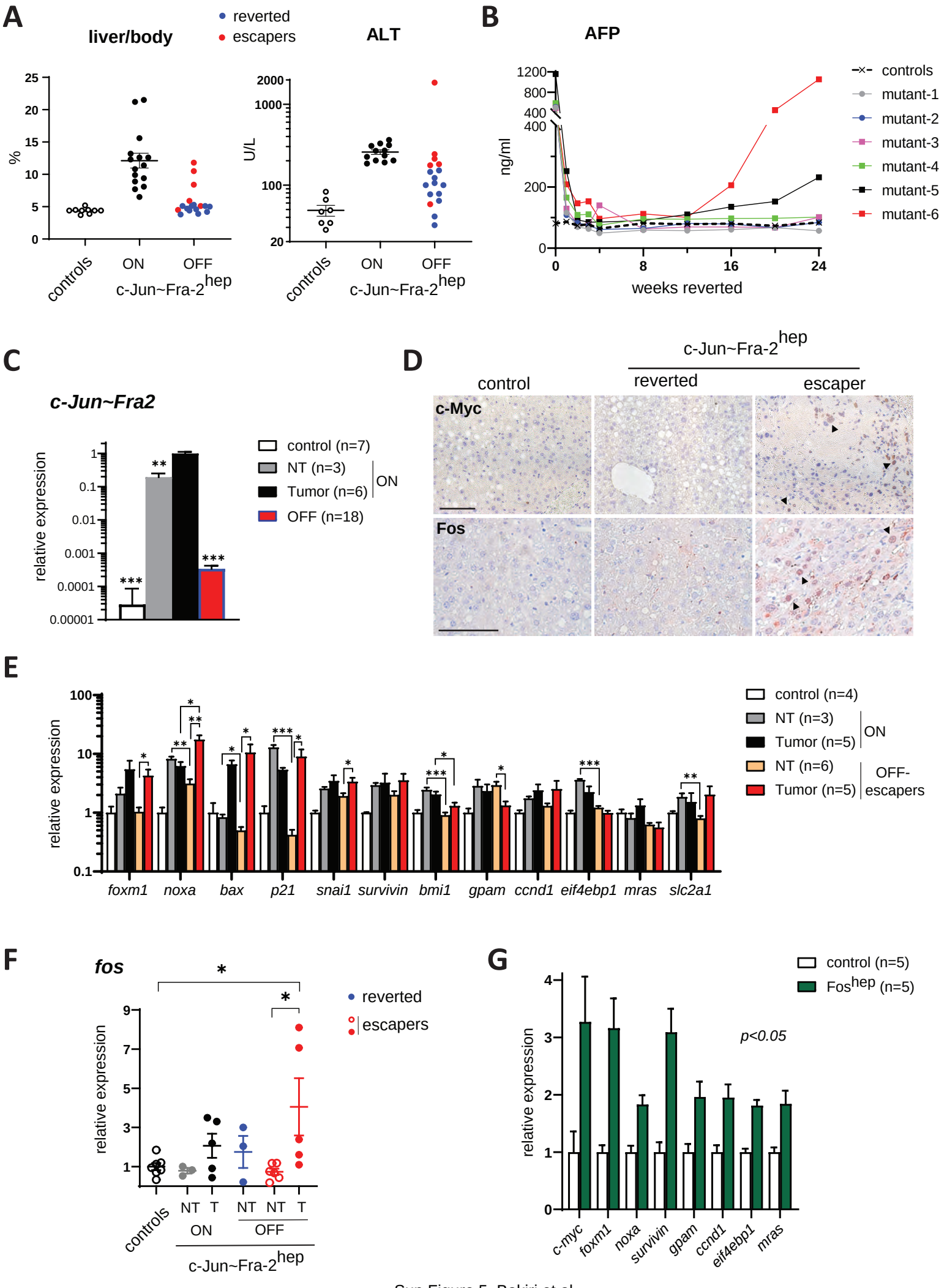

Sup Figure 5. Bakiri et al.

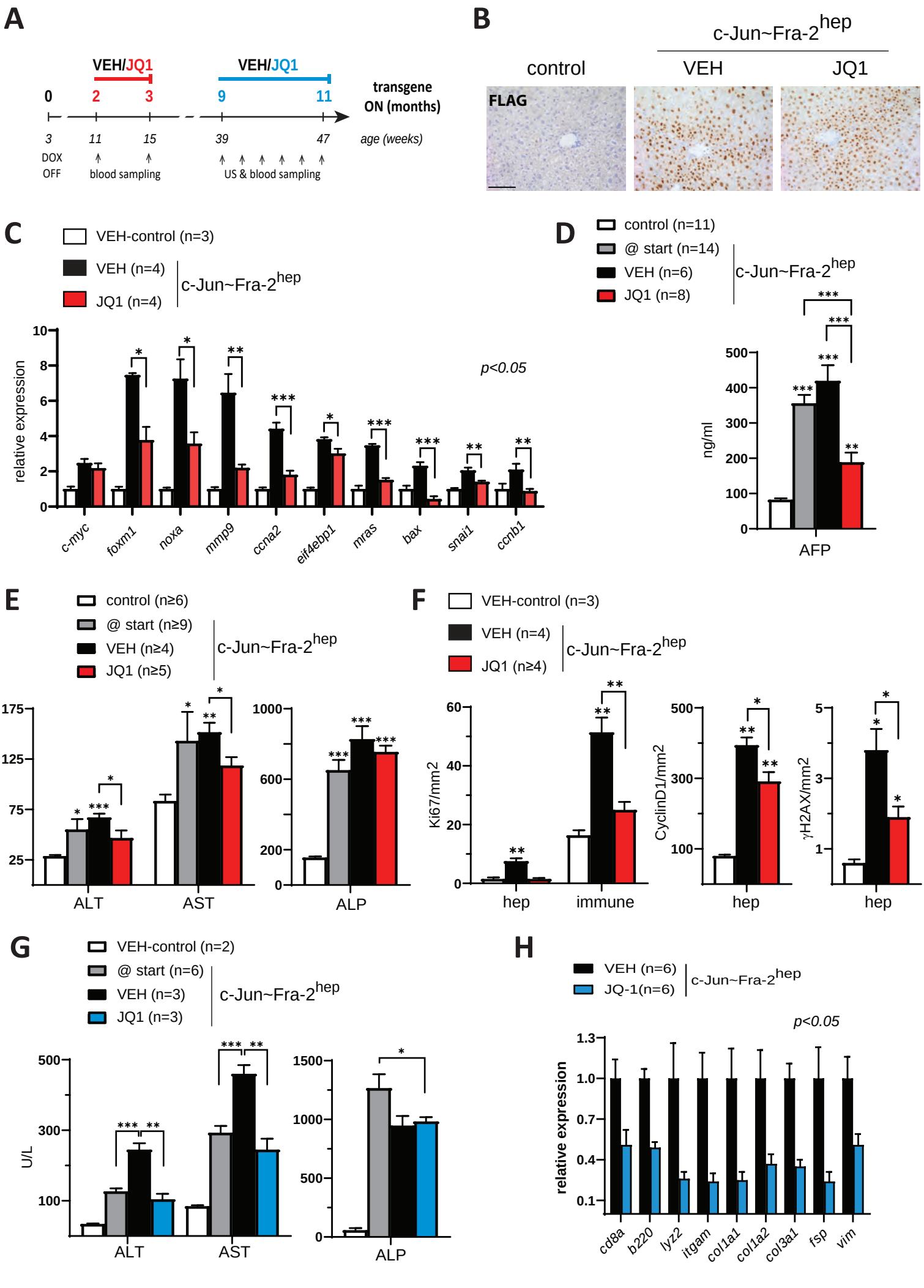

Sup Figure 6. Bakiri et al.

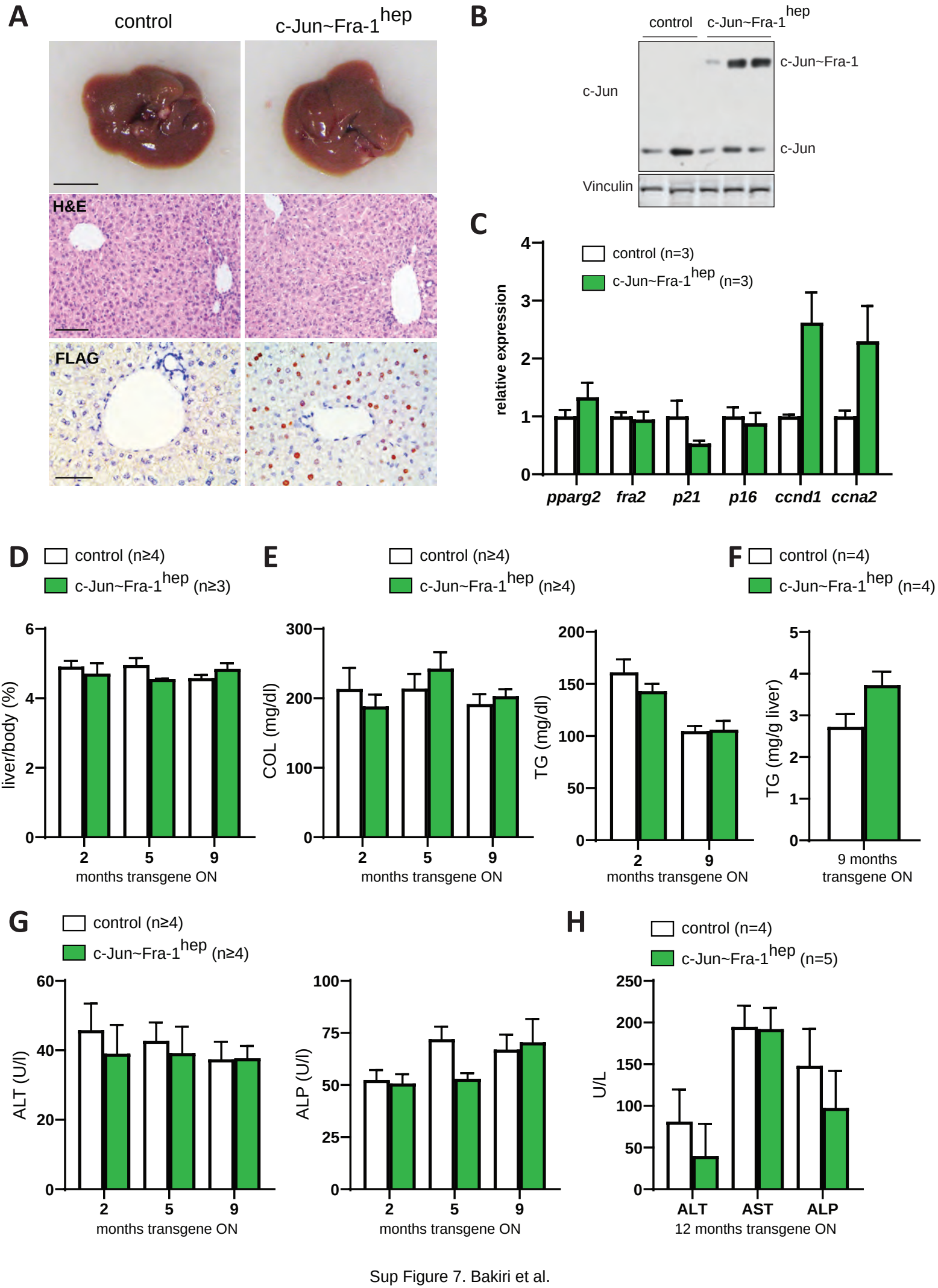

Sup Figure 7. Bakiri et al.

A

	Tumors		mean T.vol (mm3)		T.burden (mm3)		AFP (ng/ml)		ALT (U/L)		ALP (U/L)	
	start	end	start	end	start	end	start	end	start	end	start	end
mutant-1	1	-	0.4	-	0.4	-	503	57	173	31	1,168	144
mutant-2	2	-	5.5	-	10.9	-	514	84	149	77	744	188
mutant-3	2	1+1*	42.3	12.8	84.6	25.5	489	101	133	36	1,152	200
mutant-4	3	1+1*	62.0	4.4	185.9	8.9	589	102	138	84	1,008	204
mutant-5	1	2+1*	95.3	35.2	95.3	211.4	1,158	232	99	232	1,080	272
mutant-6	2	2+1*	591.5	272.6	1,183.1	1,090.3	580	1,054	208	742	948	111
control-1	*not applicable*						85	95	27	57	183	190
control-2							76	72	36	22	138	150

B

	group	Tumors		T.burden (mm3)		liver/body	AFP (ng/ml)		ALT (U/L)		AST (U/L)		ALP (U/L)	
		start	end	start	end	(%, end)	start	end	start	end	start	end	start	end
mutant-1	VEH	5	5+3*	27.1	1,320.9	12.6	583	727	91	202	326	404	1,584	780
mutant-2	VEH	1	1+3*	6.7	251.3	13.2	663	1,063	150	268	330	468	1,272	940
mutant-3	VEH	1	1+4*	3.4	127.9	9.9	540	675	138	266	348	508	1,056	1,124
mutant-4	JQ1	3	3	45.6	351.2	9.6	634	160	108	136	282	309	1,436	1,008
mutant-5	JQ1	2	2	8.8	28.1	8.3	451	136	142	106	212	248	749	1,044
mutant-6	JQ1	2	2	4.6	33.1	7.9	485	144	131	72	260	178	1,504	896
control-1	none	*not applicable*				4.4	58	74	36	28	86	88	137	190
control-2						4.4	52	53	34	34	76	108	139	170

Table S2. Oligonucleotides used in the study

Murine RT-qPCR primers

Product	**Forward primer (5'-3')**	**Reverse primer (5'-3')**
afp	GTATGGACTCTCAGGCTGCT	GAAGGGGTTCCTCCTTGACA
asma	CAATGGCTCTGGGCTCTGTA	TCATCCCCCACATAGCTGTC
b220	GGGTTGTTCTGTGCCTTGTT	GGATAGATGCTGGCGATGAT
bax	TCTGGATCCAAGACCAGG	GGACTCCAGCCACAAAGAT
bex1	CCTAACGGAGGCACCTGTT	CGCCTTGATCTTTGGACTCC
bmi1	GCTTGGCTCGCATTCATTT	GGACACACATTAAGTGGGGA
ccna2	AGAGGCAGCCAGACATCACT	AAGCTAGCAGCATAGCAGCC
ccnb1	CATAGGATACCTACCGTGTT	GTTAGCCTAAACTCAGAAGC
ccnd1	TGCTGCAAATGGAACTGCTT	GGTCTGCTTGTTCTCATCCG
cd133	TGCAGCAATCACTGAATACG	AACAGAGTCCAAAGAGGCAA
cd163	CTCTGCTGTCACTAACGCTC	GGACACTTCATTCATGCTCC
cd44	GCACTGTGACTCATGGATCC	TTCTGGAATCTGAGGTCTCC
cd68	TGATCTTGCTAGGACCGCTT	GGAGCTGGTGTGAACTGTGA
cd8a	TCAGTTCTGTCGTGCCAGTC	ATCACAGGCGAAGTCCAATC
cdk1	GTCCCTGCAGGACTACAAGA	TTGAGAGCAAATCCAAGCCG
c-fos	CCAGTCAAGAGCATCAGCAA	TAAGTAGTGCAGCCCGGAGT
c-jun	AGTCTCAGGAGCGGATCAAG	TGAGTTGGCACCCACTGTTA
c-myc	TCACCAGCACAACTACGCCG	TGCTTCAGGACCCTGCCACT
col1a1	CATGTTCAGCTTTGTGGACCT	TAGGCCATTGTGTATGCAGC
col1a2	GCTGGAATCCGAGGTCCTAA	GCCAACATTTCCAGGAGACC
col3a1	AAAGAGGATCTGAGGGCTCG	GCCACCAGACTTTTCACCTC
dlk1	TGGAGTCTGCAAGGAACCAT	TGGCAGGGAGAACCATTGAT
eif4ebp1	ACTAGCCCTACCAGCGAT	TACGGCTGGTCCCTTAAATG
fms	CATGGCCTTCCTTGCTTCTAA	TGCCGTAGGACCACACATCA
foxm1	ATTCACCCAAGTGCCAATCG	ATTGGGTCGTTTCTGCTGTG
fra-2	TGGAGTGATCAAGACCATCG	AGCTAGCTTGTTTCTCTCCC
cjun-fra2	CTCACCGCAGAAGCAGTA	TGTCGTCGTCGTCCTTGTAG
fsp	TGAGCAACTTGGACAGCAACA	TTCCGGGGTTCCTTATCTGGG
gp73	AGAAGCTCATTCGAGACCTG	CATCTGGCTGATACACTGGT
gpam	GCGGGGTCAGCACAT	AGGCTCTCCTTCCATTTCAG
gpc3	GTGACGGGATGGTGAAAGTG	TGTGAGAGGTGGTGATCTCG
h19	CCTCCCACGCAAGTTCAATT	ACCGGACCATGTCATGTCTT
il6	CAAAGCCAGAGTCCTTCAGAG	TGGTCTTGGTCCTTAGCCAC
itgam	CCAAGACGATCTCAGCATCA	TAGCAGGAAAGATGGGATGG
ly6d	AGGATGAAGACAGCTCTGC	AGAAGTAGAAGTTGGACGGG
ly6g	CATTGCAAAGTCCTGTGTGC	AGGGGCAGGTAGTTGTGTTG
lyz2	TTTAGCTCAGCACGAGAGCA	CACTGCAATTGATCCCACAG
marco	GAAGACTTCTTGGGCAGCAC	GTGAGCAGGATCAGGTGGAT
mcm2	CTTTGTACTGGGGCCTTTCT	GATGCGGATACGTTGGTAGT
mgla	CAGGAGAAATGCCAACACCT	GCGTTGTAGCCGTAGACCAT
mmp9	TCCCCAAAGACCTGAAAACC	TAGAGACTGCTTCTCTCCCA
mras	GAGAAGTCGCTCACCACT	CATGTTTCTGGTAGTCAGGC
mrc1	CACTTTCAATGCCTGGACTG	GCCACCAATCACAACTACAC
nope	GGGGTAGGGAGTGAAACCAA	CCGCCCTTTTCCTATGCAAA
noxa	GTGCACCGGACATAACTGTG	GGAGTTGAGCACACTCGT

onec	AGAGCTCCAAGAGGCTTCC	GAAAGAAGATCCAGGCCCTC
p16	CTTGGTCACTGTGAGGATTCAG	GTGAACGTTGCCCATCATCA
p19	CCAAGATGCCTCCGGTACTA	CCCTCTCTTATCGCCAGATG
p21	CAGAGTCTAGGGGAATTGGA	GTCGGACATCACCAGGATT
p53	AAGATCCGCGGGCGTAA	CATCCTTTAACTCTAAGGCCTCATTC
pdgfrA	TGGAGCTTGAGGGAGAGAAA	AGAAAGACCTGGTGGGAGGT
pdgfrB	GAGTTTGCTCTTGTCCCGAG	AGGACAGCTGTAAGGGGGTT
pparg2	GAAGTTGGTGGGCCAGAATG	TTGACCCAGAGCATGGTGC
rpl4	CTACTGCACTGGCAACCAAA	TCTTGGCAACCACCTTTTTC
rps29	ATGGGTCACCAGCAGCTCTA	GCCTATGTCCTTCGCGTACT
slc2a1	GCGGGAGACGCATAGTTA	GACACCAGTGTTATAGCCGA
snai1	CATGTCTGGACCTGGTTCCT	AAGGGTCCTTGAGGGAGGTA
sox9	GTTGATCTGAAGCGAGAGGG	CATTGACGTCGAAGGTCTCA
survivin	TGGCAGCTGTACCTCAAGAA	TCCCAGCCTTCCAATTCCTT
tgfb1	GTCCTTGCCCTCTACAACCA	GTTGGACAACTGCTCCACCT
tgfb2	CCCACATCTCCTGCTAATGT	CGAAGGCAGCAATTATCCTG
tgfbR2	GGACCCTACTCTGTCTGTGG	TGGAGTAGACATCCGTCTGC
vim	GTGCGCCAGCAGTATGAAAG	GCATCGTTGTTCCGGTTGG
Murine ChIP-qPCR primers		
Product	**Forward primer (5'-3')**	**Reverse primer (5'-3')**
myc WRE	CAGGCAAGCCCAAAGAATAG	CCCACAGCCAAATCTGAATC
myc Promoter	CTTTGACACGTCCAGCTTAC	CCTAGTTGTGGATGGGGAAA
Dusp1 promoter	TGGCAAAACCCATTGATGTC	AGAAAGGGGAAAGCGAATCT
intergenic	CAGTTCACACATATAAAGCAG	GTTGTTGTTGTTGCTTCACTG
Human RT-qPCR primers		
Product	**Forward primer (5'-3')**	**Reverse primer (5'-3')**
MYC	CACCGAGTCGTAGTCGAGGT	GCTGCTTAGACGCTGGATTT
RPL29	CTTCCGGTTCTAGGCGCTT	ATTTTCGGGACTGGTTGTGTGT
RPS29	ATGGGTCACCAGCAGCTCTA	GCCTATGTCCTTCGCGTACT

Table S3. Antibodies used in the study

Antigen	Supplier	Reference
Actin	Sigma	A4700
AFP	R&D	AF5369
AKT	Cell Signaling	9272
Bex1/2	Santa Cruz	sc-98915
Bip	Cell Signaling	3183
CD3	Roche	790-4341
Cdk1	Pharmingen	558900
Cdk2	Sigma	C5223
c-Fos	Cell Signaling	2250
c-Jun	Cell Signaling	9165
c-Myc (IB)	Santa Cruz	sc-42
c-Myc (IHC)	Abcam	ab32072
Cyclin A	Sigma	C4710
Cyclin B	Sigma	C8831
Cyclin D1 (IB)	home made	Jiri Bartek
Cyclin D1 (IHC)	DAKO	M3635
Cyclin E	Upstate	07-687
ERK1/2	Cell Signaling	9102
F4/80	Biorad	MCA497R
Flag	Sigma	F3165
Fra-2	Sigma	MABS1261
Fsp27	Novus Biologicals	NB100-430
Gapdh	Sigma	G8795
γH2AX	Millipore	05-636
GP73	Santa Cruz	sc-48011
GSK3β	Cell Signaling	9332
H2A	Cell Signaling	2578
IgG	Millipore	12-371B
JNK1/2	Cell Signaling	9252
Ki67	Dako	M7249
Mcm2	BD	610700
p19	Santa Cruz	sc-7403
p21	Abcam	ab107099
p38	Cell Signaling	9218
p53	Leica	NCL-p53-CM5p
p65	Santa Cruz	sc-372
p-AKT (308)	Cell Signaling	9275
p-AKT (473)	Cell Signaling	9271
Pax5	Santa Cruz	sc-1974
PERK	Cell Signaling	3192
p-ERK1/2	Cell Signaling	9106
p-GSK3β	Cell Signaling	9336
p-JNK1/2	Cell Signaling	9251
p-p38	Cell Signaling	9211
p-p65	Cell Signaling	3037
Pparγ	Cell Signaling	2443

p-PERK	Cell Signaling	3179
p-PTEN	Cell Signaling	9551
p-Smad2	Cell Signaling	3101
p-Stat3	Cell Signaling	9131
PTEN	Cell Signaling	9559
Smad2	Cell signaling	3103
Sox9	Millipore	AB5535
SP1	Santa Cruz	sc-059
Stat3	Cell Signaling	9132
Tubulin	Sigma	T9026
Vinculin	Sigma	V4505

Supplementary Figure legends

Supplementary Figure 1: Related to Figure 1

A. Survival of c-Jun~Fra^{hep} and control mice off Dox since weaning (*p* by Mantel-Cox Log-rank test). **B.** Liver/body weight ratio over time in c-Jun~Fra-2^{hep} mice and controls (n=control/mutant: 8/6, 4/5, 7/7). **C.** Mean number of small (≤2mm) and large (>2mm) hepatic surface nodules in c-Jun~Fra^{hep} mice at 9 months of transgene expression (n=31). Comparison of macroscopic liver lesion incidence **(D)** and serum AFP **(E)** in Fra^{hep}, c-Jun~Fra^{hep} and control mice, after 9-15 months of transgene expression (controls n=32, mutants n=9/11/17/13). **F.** Serum albumin (n=control/mutant: 8/6, 4/5, 7/7) over time in c-Jun~Fra-2^{hep} mice and controls. **G.** Serum ALT (left, n=control/mutant: 8/6, 4/5, 7/7), AST (middle, n=control/mutant: 9/13, 5/7, 8/6) and ALP (right, n=control/mutant: 8/6, 4/5, 7/7) over time in c-Jun~Fra-2^{hep} mice and controls. **H.** Immunoblot for ER stress-related proteins in liver extracts from c-Jun~Fra-2^{hep} mice (non-tumoral and tumors) and controls at 9 months of transgene expression. **I.** IHC for p21 in liver sections from c-Jun~Fra-2^{hep} mice and controls. Bar = 100μm, arrows point to positive nuclei. **J.** qRT-PCR quantification of *p21, p16, p19* and *p53* in c-Jun~Fra-2^{hep} livers compared to controls at 2 months. Tubulin is used to control immunoblot loading. Bars = means ±SEM. * p<0.05, ** p<0.01, *** p<0.001 (t-test to controls).

Supplementary Figure 2: Related to Figure 2

A. Top enriched cell cycle-related MSigDB Hallmark signatures in mutant RNAseq groups compared to their respective controls (2 months: n=6, 9 months: n=3) by GSEA. Normalized enrichment scores (NES) are shown as bars and FDR q-values (–log10) as dot plots. Data are ordered by NES in the 2 months dataset. **B.** CIBERSORTx deconvolution of hepatocyte subsets in c-Jun~Fra-2^{hep} liver RNAseq datasets (control: C, n=6, mutant: NT, n=3) at 2 months. **C.** IHC for Glutamine synthetase (GS) in liver sections from c-Jun~Fra-2^{hep} mice and controls at 2 months of transgene expression. Bar = 100μm. **D.** Immunoblot analyses of c-Jun (detecting endogenous

c-Jun and ectopic c-Jun~Fra-2) and various Cyclins and Cdks in liver extracts from c-Jun~Fra-2^{hep} mice (non-tumoral and tumors) and controls. **E.** qRT-PCR quantification of *ccna2* (encoding Cyclin A2), *cdk1* and *Il6* expression over time in c-Jun~Fra-2^{hep} tumors and non-tumoral (NT) liver areas compared to controls. **F.** IHC quantification of F4/80, Pax5 and CD3 in liver sections of c-Jun~Fra-2^{hep} mice and controls at 2 months. **G.** qRT-PCR quantification of immune-cell markers in c-Jun~Fra-2^{hep} tumors and non-tumoral (NT) liver areas compared to controls. **H.** Heat map of MSigDB C8 liver cell gene sets (AIZARANI_LIVER) enriched in each mutant group. Rows display the NES of the 27 gene sets (out of 31) that had FDR>25% in the 3 datasets, grouped by cell type. **I.** Immunoblot analyses of total and phosphorylated ERK, JNK, p38, PTEN, AKT and GSK3β in livers from c-Jun~Fra-2^{hep} mice (non-tumoral and tumors) and controls. **J.** IHC for phosphorylated Stat-3 in liver sections from c-Jun~Fra-2^{hep} mice and controls at 9 months of transgene expression. Bar = 100μm, arrows point to positive nuclei. **K.** Immunoblot for total and phosphorylated Stat3 in liver extracts from c-Jun~Fra-2^{hep} mice and controls at 2 months of transgene expression. Tubulin, Actin and Vinculin are used to control immunoblots loading. Bars = means ±SEM, n≥3. * $p<0.05$, ** $p<0.01$, *** $p<0.001$ (t-test to controls).

Supplementary Figure 3: Related to Figure 3

A. qRT-PCR quantification of fibrosis-associated genes in c-Jun~Fra-2^{hep} tumors and non-tumoral (NT) liver areas compared to controls. **B.** MSigDB Hallmark signatures for EMT (upregulated) and lipid metabolism (downregulated) in mutant RNAseq groups compared to their respective controls (2 months: n=6, 9 months: n=3) by GSEA. Normalized enrichment scores (NES) are shown as bars and FDR q-values (–log10) as dot plots. Data are ordered by NES in the 2 months dataset. **C.** Immunoblot for Pparγ and Fsp27 in liver extracts from c-Jun~Fra-2^{hep} mice and controls at 2 months. **D.** Expression of *pparg2* and selected Pparγ target genes by RNAseq in c-Jun~Fra-2^{hep} livers at 2 and 9 months (tumors and non-tumoral), each relative to their respective controls (set to 1). Mean fold change (log2) is shown and all changes except one (indicated by $) are

statistically significant after multiple testing corrections. The red dotted line marks the 2-fold change threshold. **E.** Expression of *nr1h3* (encoding LXRα) *nr1h4* (encoding FXR) and selected LXRα target genes by RNAseq in c-Jun~Fra-2^{hep} livers at 2 and 9 months (tumors and non-tumoral). Adjusted p value is plotted against mean fold change (log2) for each sample group relative to its control group. The red dotted line marks the 0.05 p value cut-off and the 2 vertical dotted lines mark the 2-fold change thresholds. **F.** Serum triglycerides (TG, n=4/4) and cholesterol (COL, n=7/7) in c-Jun~Fra-2^{hep} mice and controls at 9 months. SP1 is used to control immunoblots loading. Bars = means ±SEM, n≥3. * p<0.05, ** p<0.01, *** p<0.001 (t-test to controls).

Supplementary Figure 4: Related to Figure 4

A. c-Myc IHC (top, bar = 100μm, arrows point to positive nuclei) and immunoblot (bottom) in liver sections or extracts from c-Jun~Fra-2^{hep} mice and controls at 2 months. **B.** qRT-PCR quantification of *c-myc* expression in Fra^{hep} (n=3) and c-Jun~Fra^{hep} (n=3) livers compared to controls (n=12) at 2 months. **C.** qRT-PCR quantification of *foxm1* expression over time in c-Jun~Fra-2^{hep} tumors and non-tumoral (NT) liver areas compared to controls. **D.** qRT-PCR analyses of *c-jun*, *fra-2* and c-*myc* in livers from 4 weeks-old mice lacking *fra-2* expression in the liver (Fra-2$^{\Delta li}$) and Fra-2-proficient control littermates, 48hrs after diethylnitrosamine (DEN) injection. For each gene, expression is plotted relative to mean expression in 2 untreated controls (set to 1, dotted line). **E.** Representative liver morphology (left) and mean surface nodules quantification (right) in Fra-2$^{\Delta li}$ and control mice 9 months post-DEN (injected at 2 weeks of age). Bar = 1 cm, tumors are indicated by arrows. **F.** Serum AFP and ALT in Fra-2$^{\Delta li}$ and control mice 9 months after DEN. **G.** qRT-PCR analysis of *c-jun*, *fra-2* and c-*myc* in liver tumors from Fra-2$^{\Delta li}$ and control mice 9 months after DEN. For each gene, expression is plotted relative to mean expression in 3 untreated controls (set to 1, dotted line). **H.** Data mining using publicly available human liver-related ChIP-seq datasets: JUN, FRA2 and p300 ChIP-seq peak distribution around the c-MYC gene in human HepG2 liver cells. The red dotted box indicates the conserved c-Myc 3´enhancer

(WRE) enhancer. **I.** MYC expression in HepG2 cells either wild-type or with CRISPR knock-out of the c-MYC (WRE) enhancer after transient expression of GFP with increasing amounts of c-Jun~Fra-2 expression vectors (n=2 per point). qRT-PCR values are plotted as a ratio to GFP with MYC expression in HepG2 cells expressing only GFP set to 1. **J.** MYC qRT-PCR in HepG2 cells after siRNA knock-down of JUN genes relative to cells treated with scrambled (scr) siRNA. **K.** Correlation plots for JUN, FRA2 and MYC mRNA expression in human HCC patients using publicly available (TCGA) datasets (n=365). Fragments Per Kilobase of transcript per Million mapped reads (FPKM) are plotted. In the plot on the right side, samples with high JUN and FRA2 (HH, n=136) or low JUN and FRA2 (LL, n=99) are shown in red and grey, respectively (cut off = 30.55 for Jun and 4.03 for FRA2). **L.** MYC, FOXM1 and CCND1 (encoding for Cyclin D1) expression in HH and LL patients (Mann-Whitney test). **M.** TCGA score stratification of Overall Survival comparing HH to LL patients (*p* by Mantel-Cox Log-rank test). Tubulin is used to control immunoblot loading. Bars/dots = means ±SEM. * $p<0.05$, ** $p<0.01$, *** $p<0.001$ (t-test to controls).

Supplementary Figure 5: related to Figure 5

A. Liver to body weight (left) ratio and Serum ALT (right) at endpoint in un-reverted (9 months ON) and reverted (OFF, 9 months ON then 6 months OFF) c-Jun~Fra-2^{hep} and control mice. Reversion escapers are marked in red. **B.** Serum AFP over time in 6 mutants subjected to the reversion protocol and longitudinal US monitoring. **C.** qRT-PCR quantification of c-Jun~Fra-2 in liver samples (tumoral and non-tumoral) from c-Jun~Fra-2^{hep} mice at the OFF endpoint compared to non-tumoral (NT) liver areas and tumors (set to 1) from un-reverted (ON) c-Jun~Fra-2^{hep} mice. **D.** c-Myc and c-Fos IHC in liver sections or extracts from c-Jun~Fra-2^{hep} mice and controls at endpoint of the reversion protocol. Arrows point to positive nuclei. Bar = 100μm. **E.** qRT-PCR quantification of a selection of c-Myc target genes in tumors and non-tumoral (NT) liver areas from c-Jun~Fra-2^{hep} mice either un-reverted (ON) or with tumors that escaped reversion (OFF) relative to (pooled) controls. **F.** qRT -PCR for *fos* in tumors (T) and non-tumoral (NT) liver areas from un-

reverted (ON) and reverted (OFF) c-Jun~Fra-2^{hep} mice compared to controls. Mice with reversion escapers are plotted separately (red). **G.** qRT-PCR quantification of *c-myc* and c-Myc target genes in the livers of in Fos^{hep} mice livers compared to controls at 2 months, $p<0.05$ for each mRNA. Bars/dots = means ±SEM. * $p<0.05$, ** $p<0.01$, *** $p<0.001$ (t-test).

Supplementary Figure 6: related to Figure 6

A. Experimental design and timeline of the therapeutic trials. US: Ultrasonography. **B-E.** c-Jun~Fra-2^{hep} mutants with 2 months of transgene expression (off Dox at weaning) were randomized and treated with JQ1 or vehicle (VEH, during 4 weeks. **B.** Flag IHC in liver sections from c-Jun~Fra-2^{hep} mice treated with JQ1 or VEH compared to controls. Bar = 100μm. **C.** qRT-PCR for c-Myc & c-Myc target genes in livers from c-Jun~Fra-2^{hep} mice treated with JQ1 or VEH compared to VEH-treated controls. $p<0.05$ between VEH-treated mutants and controls for all genes. Serum AFP (**D**), ALT, AST and ALP (**E**), in c-Jun~Fra-2^{hep} mice 2 months after transgene induction (start) and after 4 weeks of JQ1 or VEH treatment. 3 VEH-treated and at least 3 untreated control mice are included as healthy reference. **F.** IHC quantification of Ki67 in hepatocytes (hep) and immune cells and of Cyclin D1 and γH2AX in hepatocytes using liver sections of VEH-treated controls and VEH or JQ1-treated c-Jun~Fra-2^{hep} mice. **G.** Serum ALT, AST and ALP at start and endpoint in c-Jun~Fra-2^{hep} mutants with 9 months of transgene expression (off Dox at weaning) and treated with JQ1 or VEH during 2 months. 2 VEH-treated control mice are included as healthy reference. **H.** qRT-PCR quantification of immune- and fibrosis-related genes at endpoint in liver samples comparing VEH- and JQ1-treated (responsive) c-Jun~Fra-2^{hep} mice. Bars = means ±SEM. In dot plots and graphs, means ±SEM are plotted. *: $p<0.05$, ** $p<0.01$, *** $p<0.001$ (t-test).

Supplementary Figure 7: related to Methods

A. Liver morphology, histology (H&E, middle) and Flag IHC (bottom) in a c-Jun~Fra-1^{hep} and control mouse. Bar = 1 cm (top) and 100μm (middle and bottom). **B.** Immunoblot analyses of c-

Jun (detecting endogenous c-Jun and ectopic c-Jun~Fra-1) in liver extracts from c-Jun~Fra-1^{hep} mice and controls at 5 months. **C.** qRT-PCR quantification of *pparg2, fra-2, p21, p16, ccnd1* (encoding Cyclin D2) and *ccna2* (encoding Cyclin A2) in c-Jun~Fra-2^{hep} livers compared to controls at 2 months. Vinculin is used to control immunoblot loading. **C.** Liver/body weight ratio over time in c-Jun~Fra-1^{hep} mice and controls. **D.** Serum cholesterol (left) and triglycerides (right) over time in c-Jun~Fra-1^{hep} mice and controls. **F.** Liver triglycerides content in c-Jun~Fra-1^{hep} mice and controls at 9 months. **G.** Serum ALT (left) and ALP (right) over time in c-Jun~Fra-1^{hep} mice and controls. **H.** Serum ALT, AST and ALP in c-Jun~Fra-1^{hep} mice and controls at 12 months.

Supplementary Table 1: related to Figure 5

Summary of ultrasound and blood parameters at start and endpoint in **(A)** 6 mutants and 2 controls subjected to the reversion protocol with blood and ultrasound follow up depicted in Figure 5. Neo-tumors are indicated with an asterisk. **(B)** 6 mutants treated with either JQ-1 or vehicle with blood and ultrasound follow up depicted in Sup Figure 6. Neo-tumors in VEH-treated mutants are indicated with an asterisk and tumor burden values at end point include these tumors.

Supplementary Table 2: related to Methods

Primers used in the study.

Supplementary Table 3: related to Methods

Antibodies used in the study.

Supplementary Materials and Methods

Mice and treatments

Jun~Fra-2^{hep}, Fra-1^{hep}, Fra-2^{hep}, Fos^{hep}, Fra-2$^{\Delta li}$ mice were previously described (1-3). The tet-switchable Col1a1::TetOP-Jun~Fosl1 allele, that was combined to the LAP-tTA allele (MGI:3056818) to generate Jun~Fra-1^{hep} mice, was generated with the CNIO Mouse Genome

Editing Core Unit according to (4) and similar to the other tet-switchable AP-1 alleles (MGI:5586533, MGI:5585716, MGI:5585642, MGI:5555845) used in this study. Additional data related to the analysis of Jun~Fra-1^{hep} mice can be found in Suppl. Figure 7. Mice were backcrossed and maintained on pure C57BL/6J background and male mice were used for all experiments. Liver samples from c-Jun$^{\Delta li}$; HBV^{tg} mice used in this study were generated in a previously published study (5). Randomized block design was used to organize the experimental cohorts and littermates used as controls. Mice were housed in Specific Pathogen-Free environment with free access to food and drink. Dox (1g/l, Sigma-Aldrich) was supplied in sucrose-containing (100g/l) drinking water to breeding cages and experimental cohorts weaned on normal drinking water (OFF dox). 2 week-old pups or 8 week-old mice were injected intraperitoneally with 25 or 100 mg/kg DEN (Sigma-Aldrich) and sacrificed 9 months or 48 hours after DEN injection, respectively. JQ-1 (Abmole, M2167) was dissolved in 10% (2-Hydroxypropyl)-β-cyclodextrin (Abmole, M4893) and mice received a daily dose of 25mg/kg or an equal volume of vehicle by intraperitoneal injection. Sorafenib (Abmole, M3026) was dissolved in a 1:1 mixture of 95% ethanol and Cremophor EL (Sigma, 238470-1SET) and mice received a daily dose of 10mg/kg or an equal volume of vehicle by oral gavage. Liver tumors were detected and measured longitudinally by the CNIO imaging unit with a micro-ultrasound system (Vevo 770, Visualsonics) and an ultrasound transducer of 40 MHz (RMV704, Visualsonics). Mice were anesthetized with a continuous flow of 1% to 3% isoflurane in 100% oxygen at a rate of 1.5 liter/min on a heated bed to prevent hypothermia and abdominal hair was removed using a depilatory cream. Tumor size was calculated as 4/3xπxAxBxC, where A, B, and C are the lengths of the three semi-axes of the tumor. All animal experiments were performed in accordance with institutional, national, and European guidelines for animals used in biomedical research and approved by the Spanish National Cancer Research Centre (CNIO) Institutional Animal Care and Use Committee and the CNIO–Instituto de Salud Carlos III Ethics Committee for Research and Animal Welfare and the

Austrian Federal Ministry of Education, Science and Research (approved project Wagner E. 171/18).

Blood and liver chemistry analyses

Blood was collected by submandibular vein or cardiac (experimental endpoint) puncture. Routine blood measurements were performed using a VetScan (Abaxis) or a Reflovet Plus (Scil Diagnostics) blood chemistry analysers. AFP & PIVKA were measured on serum samples by ELISA (R&D, MAFP00 and FineTest, EM1857, respectively). For liver Triglyceride content, 25-75mg of liver tissue was homogenized in chloroform/methanol (8:1 v/v; 500ul per 25 mg tissue) and shaken at RT for 8-16 hours. H_2SO_4 was added to a final concentration of 0.28M and the lower phase collected after centrifugation, dried, and Triglycerides measured using an enzymatic assay kit (Cayman Chemicals,10010303).

Histology

Tissues were frozen in OCT (Tissue-tek) or fixed in 4% formalin and embedded in paraffin and 4µm sections prepared. Standard procedures were used for H&E-, Masson's trichrome and Oil-red-O stainings. IHC was performed either by the CNIO Histopathology Core Unit or manually as previously described (1, 3) using matching secondary antibodies from the Vectastain Elite ABC kits (Vector Laboratories) and Carazzi's hematoxylin (Panreac AppliChem) counterstaining. Quantification was performed on digital scans using Panoramic Viewer (3DHistech) and ImageJ softwares. Antibodies are listed in Suppl. Table 3.

Protein isolation, Immunoblot and Chromatin immunoprecipitation

Small pieces of fresh or snap frozen livers were disrupted using a Precellys device (Bertin Technologies) in RIPA buffer (50 mM Tris, pH 7.4, 150 mM NaCl, 1% NP-40, 0.5% Na-deoxycholate, and 0.1% SDS). Protein lysates were quantified using a BCA protein assay reagent (Thermo Fisher Scientific). Immunoblot analysis was performed using standard protocols as

described (2, 3). Chromatin immunoprecipitation (ChIP) on murine liver samples was performed as detailed in (2) and quantitative PCR (qPCR) was used to quantify amplified fragments using GoTaq qPCR Master Mix (Promega) and Eppendorf fluorescence thermocyclers with duplicate reactions. The $2^{\Delta\Delta CT}$ method was used to quantify amplified fragments in the Input and ChIP fractions and calculate input recovery in each condition. ChIP-qPCR primers and ChIP antibodies are listed in Suppl. Table 2 and Suppl. Table 3, respectively.

Cell culture and in vitro experiments

Murine AML12 and human HepG2 liver-derived cell lines were maintained in DMEM supplemented with 10% FBS at 37°C and 5% CO2. To delete the c-MYC (WRE) enhancer, two flanking CRISPR guides were designed (sg_1: GCCCCTTTGTGGCCTAGGGC and sg_2: GCCCTAGGCCACAAAGGGGC) and cloned into the lentiCRISPR v2 backbone containing a puromycin selection cassette (Addgene#52961) and the resulting plasmid transfected in HepG2 cells using Xtreme gene (Sigma). Cells underwent selection for 48 hours before isolation and expansion of single clones. CRISPR-edited clones were identified by genotyping PCR (primers: For: TTGGCACGTCATAT and Rev: GAGCTTGGCTATGGG) and deletion of the CRISPR-targeted region confirmed by sequencing. Guides and genotyping primer sequences can be found in Suppl. Table 2. AML12 cells (1.25×10^5 cells/well in a 24 well plate) were transfected in technical quadruplicates using Lipofectamine 2000 (Invitrogen) with 0.05µg Renilla vector (pHRG-tk, Promega), 0.5µg c-Myc 3´enhancer luciferase reporter (6) and 1µg of pBabe-Fra-2, pBabe-Jun~Fra-2, or emtpy pBabe (control) expression vectors (7). Luciferase activity was measured 48 hours later using the Dual-Glo Luciferase Assay (Promega) and a Szabo Scandic luminometer following the manufacturer´s recommendations. AML12 cells (3×10^5 cells/well in a 6 well plate) were transfected in technical duplicates using Lipofectamine 2000 (Invitrogen) with 1µg of pBabe-Fra-2, pBabe-Jun~Fra-2, or emtpy pBabe (control) expression vectors and cells harvested for RNA preparation and endogenous *c-myc* qRT-PCR 72 hours later. HepG2 cells (0.75×10^5

cells/well in a 24 well plate) were transfected using ON-TARGETplus JUN, JUNB and JUND or scramble siRNAs (Dharmacon) and Lipofectamine RNAiMAX (Thermofisher) transfection reagent and cells harvested 72 hours later for RNA preparation and endogenous MYC and RPL29 (housekeeping) qRT-PCR. Wild-type and c-MYC (WRE) CRISPR-KO HepG2 cells (1×10^5 cells/well in a 24 well plate) were transfected in technical duplicates using Lipofectamine 2000 (Invitrogen) with 0.025μg of pBabe-GFP, 0, 0.25, 0.5 or 1μg of pBabe-Jun~Fra-2 and 1, 0.5, 0.75 or 0μg of empty pBabe (control) expression vectors (1.025 μg total DNA per well) and cells harvested 48 hours later for RNA preparation and qRT-PCR for GFP, to adjust for transfection efficiency between all wells, RPL29 (housekeeping) and endogenous MYC. Primer sequences can be found in Suppl. Table 2.

RNA isolation and quantitative reverse transcription-PCR (qRT-PCR)

Total RNA was isolated using TRI Reagent (Sigma-Aldrich), complementary DNA was synthesized using Ready-To-Go-You-Prime-First-Strand Beads (GE Healthcare) or GoScript™ Reverse Transcription Mix, Oligo(dT) (Promega) and quantitative PCR was performed using GoTaq qPCR Master Mix (Promega) and Eppendorf fluorescence thermocyclers with duplicate reactions and two housekeeping genes (Rpl4 and Rps29) per run. The $2^{\Delta\Delta CT}$ method was used to quantify amplified fragments. Primer sequences can be found in Suppl. Table 2.

Bulk RNA-seq, data analysis and datamining

RNA integrity of total RNA isolated using TRI Reagent (Sigma-Aldrich) was evaluated using an Agilent 2100 Bioanalyzer (Agilent Technologies) and samples with integrity score >8 were used for bulk RNA-seq. RNA processing was performed using TruSeq RNA Sample Preparation kit (Illumina, 15031047) at the CNIO Genomic Core Unit. The resulting purified cDNA library was applied to an Illumina flow cell for cluster generation (TruSeq cluster generation kit v5) according to the manufacturer's protocols and sequenced on an Illumina HiSeq2000 instrument at the Vienna BioCenter Core Facilities NGS Unit. RNA-seq reads (average 24 million reads per sample)

were converted from .bam to .fastq format using bedtools v2.27.1 (8) at the MUV Genomics Core Facility. Reads in fastq format were aligned to the mouse reference genome (GRCm38/mm10) with Gencode mV23 annotations using STAR aligner (9) version 2.6.1a in 2-pass mode. Raw reads per gene were counted by STAR. TPM were generated by RSEM (10). Differential gene expression was calculated using DESeq2 (11) version 1.22.2 with Benjamini-Hochberg adjusted p-values. Differentially expressed genes (1< log2foldchange<-1) with an adjusted P value of < 0.05 were considered statistically significant. RNA-seq datasets are deposited in NCBI's Gene expression omnibus archive Omnibus and are accessible through GEO Series accession no. GSE261005. Differentially expressed genes were explored by Gene Set Enrichment Analysis (GSEA) (12) using the GSEA software and gene sets downloaded from the Molecular Signature Database (www.gsea-msigdb.org/gsea/msigdb/). P-values and the false discovery rate (FDR) for the enrichment score of each gene set were calculated based on 1000 gene set permutations and statistical significance (nominal P value) of the Enrichment Score calculated using an empirical phenotype-based permutation test. Over-representation (ORA) analysis was conducted on WebGestalt (13) by uploading differentially expressed gene lists to the web server (//www.webgestalt.org) and selecting Pathways/Reactome and Gene Ontology/Biological processes as Method/Functional database for analyses with advanced parameters set to default. Enriched categories were ranked based on FDR and then the top 7 most significant categories selected for plotting. Published murine hepatocyte and myeloid single cell reference matrix files (14) were retrieved and uploaded to the CIBERSORTx webserver (www.cibersortx.stanford.edu/), together with raw gene expression counts from individual bulk RNA-Seq datasets prepared following CIBERSORTx (15) guidelines. The Impute Cell Fractions module was utilized to estimate cell type abundancies in individual samples from each dataset with Absolute mode, S-mode batch correction, 500 Permutations and Disable quantile normalization options checked. Genome-wide of HepG2 hepatoma cells (16) ChIP-seq datamining was performed using the ENCODE portal (www.encodeproject.org) and ChIP-seq traces around the c-MYC gene retrieved

from experiments ENCSR000EEK, ENCSR000BHP and ENCSR000BLW corresponding to ChIP for JUN, FRA2 and P300, respectively. The TCGA-LIHC Cancer Genome Atlas (17) treatment-naïve HCC patients clinical data (OS) and the corresponding JUN, FRA2, MYC, FOXM1 and CCND1 normalized RNAseq data from surgical resection specimens were retrieved from the Human Protein Atlas Portal (www.proteinatlas.org/).

Statistics

Methods for statistical evaluation of RNA-seq data are indicated above. For the rest of the data and unless otherwise specified, data in plots and bar graphs are presented as mean ± SD and statistical significance determined using unpaired two-tailed Student's t test, except for Kaplan–Meier plots where Mantel–Cox log-rank was used, values of $P < 0.05$ were considered statistically significant.

Supplementary References (related to Methods)

1. S. C. Hasenfuss, L. Bakiri, M. K. Thomsen, R. Hamacher, E. F. Wagner, Activator Protein 1 transcription factor Fos-related antigen 1 (Fra-1) is dispensable for murine liver fibrosis, but modulates xenobiotic metabolism. *Hepatology* **59**, 261-273 (2014).
2. S. C. Hasenfuss *et al.*, Regulation of steatohepatitis and PPARgamma signaling by distinct AP-1 dimers. *Cell Metab* **19**, 84-95 (2014).
3. L. Bakiri *et al.*, Liver carcinogenesis by FOS-dependent inflammation and cholesterol dysregulation. *J Exp Med* **214**, 1387-1409 (2017).
4. C. Beard, K. Hochedlinger, K. Plath, A. Wutz, R. Jaenisch, Efficient method to generate single-copy transgenic mice by site-specific integration in embryonic stem cells. *Genesis* **44**, 23-28 (2006).
5. C. Trierweiler *et al.*, The transcription factor c-JUN/AP-1 promotes HBV-related liver tumorigenesis in mice. *Cell Death Differ* **23**, 576-582 (2016).
6. G. S. Yochum, R. Cleland, R. H. Goodman, A genome-wide screen for beta-catenin binding sites identifies a downstream enhancer element that controls c-Myc gene expression. *Mol Cell Biol* **28**, 7368-7379 (2008).
7. L. Bakiri, K. Matsuo, M. Wisniewska, E. F. Wagner, M. Yaniv, Promoter specificity and biological activity of tethered AP-1 dimers. *Mol Cell Biol* **22**, 4952-4964 (2002).
8. A. R. Quinlan, I. M. Hall, BEDTools: a flexible suite of utilities for comparing genomic features. *Bioinformatics* **26**, 841-842 (2010).
9. A. Dobin *et al.*, STAR: ultrafast universal RNA-seq aligner. *Bioinformatics* **29**, 15-21 (2013).
10. B. Li, C. N. Dewey, RSEM: accurate transcript quantification from RNA-Seq data with or without a reference genome. *BMC Bioinformatics* **12**, 323 (2011).
11. M. I. Love, W. Huber, S. Anders, Moderated estimation of fold change and dispersion for

RNA-seq data with DESeq2. *Genome Biol* **15**, 550 (2014).
12. A. Subramanian *et al.*, Gene set enrichment analysis: a knowledge-based approach for interpreting genome-wide expression profiles. *Proc Natl Acad Sci U S A* **102**, 15545-15550 (2005).
13. Y. Liao, J. Wang, E. J. Jaehnig, Z. Shi, B. Zhang, WebGestalt 2019: gene set analysis toolkit with revamped UIs and APIs. *Nucleic Acids Res* **47**, W199-W205 (2019).
14. R. Carlessi *et al.*, Single-nucleus RNA sequencing of pre-malignant liver reveals disease-associated hepatocyte state with HCC prognostic potential. *Cell Genom* **3**, 100301 (2023).
15. A. M. Newman *et al.*, Determining cell type abundance and expression from bulk tissues with digital cytometry. *Nat Biotechnol* **37**, 773-782 (2019).
16. E. C. Partridge *et al.*, Occupancy maps of 208 chromatin-associated proteins in one human cell type. *Nature* **583**, 720-728 (2020).
17. C. G. A. R. Network., Comprehensive and Integrative Genomic Characterization of Hepatocellular Carcinoma. *Cell* **169**, 1327-1341 e1323 (2017).